

Three-Dimensional Quantitative Structure–Activity Relationship Analyses of RGD Mimetics as Fibrinogen Receptor Antagonists

Masahiro Miyashita,^a Miki Akamatsu,^{a,*} Yoshio Hayashi^b and Tamio Ueno^a

^aGraduate School of Agriculture, Kyoto University, Kyoto 606-8502, Japan

^bDepartment of Medicinal Chemistry, Kyoto Pharmaceutical University, Kyoto 607-8414, Japan

Received 14 December 1999; accepted 7 February 2000

Abstract—In order to better understand the structural requirements of fibrinogen receptor antagonists, variations in the platelet aggregation inhibitory activity of a series of RGD mimetics were examined using techniques for the analysis of three-dimensional quantitative structure–activity relationship, such as CoMFA. © 2000 Elsevier Science Ltd. All rights reserved.

Introduction

Platelet aggregation is critical in thrombus formation and is mediated by the binding of fibrinogen to its receptor, platelet-membrane glycoprotein (GP) IIb/IIIa.¹ It is known that the receptor has a specific requirement for the Arg-Gly-Asp (RGD) sequence of fibrinogen.² Therefore, RGD-containing peptides antagonize the fibrinogen binding to GPIIb/IIIa resulting in the inhibition of platelet aggregation.

Previous work examined the activities of a series of RGD mimetics, containing a variety of cationic structures, in terms of the inhibition of fibrinogen-receptor binding.³ These data generally correlated with the ionic interaction energy calculated with a model system for ligands and receptors. A distance factor evaluated in the molecule also appeared to improve the correlation. The inhibitory activity for platelet aggregation of another series of RGD mimetics has recently been reported.^{4–6} Most compounds in this series contain an amidino- or guanidinophenyl group and a piperidine-4-acetic acid. The goal of this study is to better understand the structural requirements of fibrinogen receptor antagonists. Thus, variations in the inhibitory activity of the series of compounds were examined using Comparative Molecular Field Analysis (CoMFA),⁷ Hydrophobic Interaction (HINT),⁸ and Comparative Molecular Similarity Indices Analysis (CoMSIA).⁹ CoMFA, HINT, and

CoMSIA are techniques for the analysis of three-dimensional quantitative structure–activity relationships (3D QSAR). We discuss specific chemical structures and conformations involved in the receptor binding of fibrinogen antagonists based upon the steric, electrostatic and/or hydrophobic regions surrounding the molecular series, as indicated by 3D QSAR analyses.

Methods

Compounds and activity

Compounds **16–21**, **24**, **35–57** and **59–63** were racemic at a position β to the carbonyl group adjacent to the piperidine ring. Since the *R*-enantiomer of compound **58** was 140-fold more active than the *S*-enantiomer,⁶ the potency of racemic mixtures was attributed to the *R*-enantiomer. However, compounds **16–21** and **24** have an oxygen atom at the position analogous to the carbon atom at R₄ in the **35–63** series. Therefore, the *S*-enantiomer in compounds **16–21** and **24** is homologous to the *R*-enantiomer in compounds **35–63**. Hence, for 3D QSAR studies we used the 3D structures of the *S*-enantiomers of compounds **16–21** and **24**, and the *R*-enantiomers of **35–57** and **59–63**. The activity, IC₅₀ (the 50% inhibitory concentration for platelet aggregation induced by collagen, M) values of the compounds are cited from prior reports.^{4–6} The log IC₅₀ values, pIC₅₀ were taken as an index of activity. However, the activity for racemic compounds was modified by the addition of the asymmetry factor, log 2, to the experimentally measured value. For compound **58**, the structure and activity of the *R*-enantiomer were used for the analysis. The

*Corresponding author. Tel.: +81-75-753-6489; fax: +81-85-753-6489; e-mail: akamatsu@kacs.kyoto.u.ac.jp

modified pIC_{50} values, along with the structures of compounds are listed in Tables 1–3.

Molecular modeling

The 3D structures of the compounds in this study were generated by the molecular modeling software package SYBYL, ver 6.5.3.¹⁰ The structures of compounds **1–15** and **36** were assembled, based on the low-energy conformation obtained by a systematic search in SYBYL which was applied to all rotatable bonds. The initial structures of compounds **16–35** and **37–83** were constructed based on the optimized structure of compound **36**, as a result of the systematic search. The structures were then minimized using molecular mechanics calculations performed with Tripos force field. A SAR study using conformationally fixed RGD mimetics indicated that the optimum distance between the center carbon atoms of the guanidino and carboxylate groups should be roughly 15–16 Å.¹¹ In the calculation of systematic search and energy-minimization, the distance constraint was assigned between the center carbon atoms of the amidino and carboxylate groups to be greater than 12 Å since cationic and anionic groups are strongly attractive. The structure, as minimized by molecular mechanics, was fully optimized by the semiempirical molecular orbital method, (PM3).¹² For the optimized coordinates of all compounds, atomic charges were calculated using

MNDO.¹³ The molecular electrostatic potentials of the molecules were computed from the MNDO atomic charges and used in the CoMFA and CoMSIA studies.

Structural alignment

For the 3D-QSAR model, compound **36** was selected as the template molecule for alignment because this compound has relatively high potency and a fairly fixed conformation. The center carbon atoms of the amidino and carboxylate groups, and the carbon atoms adjacent to both the benzene and piperidine rings were taken to be the key atoms for alignment (Fig. 1).

CoMFA

The analyses were done with the 'Advanced CoMFA' module of SYBYL. The aligned set of active conformers were placed in an automatically created lattice of $23 \times 27 \times 22$ Å ($X = -13$ to 11 , $Y = -15$ to 12 , $Z = -9$ to 13) with 2 Å spaces. The steric and electrostatic field energies were calculated using an sp^3 carbon probe atom with a +1 charge at all lattice intersections. The data matrix was analyzed by the partial least squares (PLS) method. We initially selected the number of compounds in the set as the number of the cross-validations and then performed the analysis using the optimum number of latent variables, deduced from the cross-validation tests

Table 1. Structure and inhibitory activity for platelet aggregation of various RGD mimetics

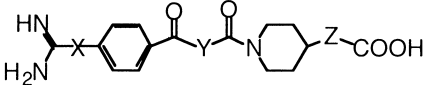
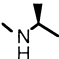
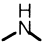
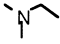
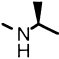

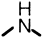
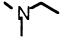

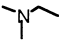
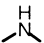
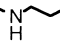
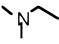

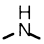
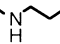

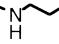
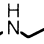
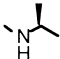
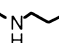

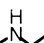
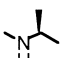

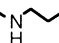

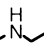
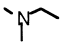
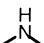
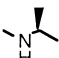

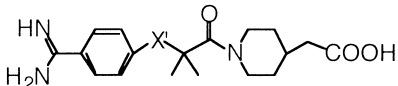
											
No.	X	Y	Z	pIC_{50}		No.	X	Y	Z	pIC_{50}	
				Obsd	Calcd					Obsd	Calcd
1	—		—	3.96	3.38	9			—	4.00	3.93
2	—			4.52	4.87	10				3.12	3.74
3	—		—	3.48	3.45	11			—	3.12	3.81
4	—			5.12	4.77	12				3.70	4.02
5	—		—	4.48	4.43	13			—	3.15	3.56
6	—			5.60	4.84	14				4.04	4.33
7	—			4.74	4.56	15			—	4.28	3.82
8				3.13	3.67						

Table 2. Structure and inhibitory activity for platelet aggregation for the compounds having a modified backbone.


No	<i>X'</i>	pIC ₅₀		No.	<i>X'</i>	pIC ₅₀	
		Obsd	Calcd			Obsd	Calcd
16		6.90	6.53	22		6.68	6.09
17		6.89	6.55	23		3.22	5.02
18		6.87	6.57	24		6.62	5.62
19		6.44	6.47	25		5.46	5.98
20		6.10	6.37	26		6.20	6.04
21		6.52	6.08				

without actual cross-validation. The inhibitory activity for platelet aggregation of the compounds in Tables 1–3 was analyzed based on the alignments described above.

HINT

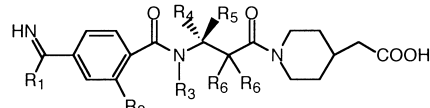
The HINT (ver 2.30) hydrophobicity fields were incorporated into CoMFA to evaluate hydrophobic interactions as a component of 3D QSAR. The analytical conditions were identical with those used for the CoMFA study.

CoMSIA

The analyses were done with CoMSIA of the 'QSAR' module of SYBYL. Similar to the usual CoMFA approach, a data table was constructed from similarity indices calculated via a common probe atom which was placed at the intersections of a regularly spaced lattice (2 Å). The probe atom has the following characteristics, charge +1, radius 1 Å, and hydrophobicity +1. The attenuation factor, α , which is the coefficient of the squared mutual distance in the Gaussian-type function in the calculation of similarity indices, was set at 0.3. The statistical evaluation for the CoMSIA analyses were performed in the same manner as described for CoMFA.

Results and Discussion

The obtained QSAR equations for the inhibitory activity for platelet aggregation are listed in Table 4. In these equations, *n* represents the number of the compound, *s*

Table 3. Inhibitory activity for platelet aggregation for compounds containing various β -amino acids


No.	R ₁	R ₂	R ₃	R ₄	R ₅	R ₆	pIC ₅₀	
							Obsd	Calcd
27	NH ₂	H	H	H	Me	H	5.30	5.82
28	NH ₂	H	H	H	phenyl	H	5.28	5.04
29	NH ₂	H	H	H	<i>i</i> -Pr	H	5.04	5.43
30	NH ₂	H	H	COO-cHex	H	H	5.72	4.68
31	NH ₂	H	H	COO-Ph	H	H	5.39	4.80
32	NH ₂	H	H	CH ₂ COOH	H	H	4.48	4.19
33	NH ₂	H	H	H	H	CH ₃	6.24	6.10
34	NH ₂	H	Me	H	H	H	5.19	4.65
35	NH ₂	H	H	phenyl	H	CH ₃	6.94	6.96
36	NH ₂	H	H	Me	H	CH ₃	7.39	7.10
37	NH ₂	H	H	Et	H	CH ₃	7.37	7.35
38	NH ₂	H	H	<i>n</i> -Pr	H	CH ₃	7.39	7.36
39	NH ₂	H	H	<i>i</i> -Pr	H	CH ₃	7.12	7.28
40	NH ₂	H	H	2-propenyl	H	CH ₃	7.07	7.10
41	NH ₂	H	H	<i>n</i> -Bu	H	CH ₃	7.39	7.33
42	NH ₂	H	H	<i>i</i> -Bu	H	CH ₃	7.39	7.48
43	NH ₂	H	H	<i>n</i> -pentyl	H	CH ₃	7.10	7.20
44	NH ₂	H	H	2-phenylethyl	H	CH ₃	7.10	7.23
45	NH ₂	H	H	2-naphthyl	H	CH ₃	6.72	6.80
46	NH ₂	H	H	4-Cl-phenyl	H	CH ₃	6.48	6.91
47	NH ₂	H	H	4-OH-phenyl	H	CH ₃	6.96	6.96
48	NH ₂	H	H	3-Cl-phenyl	H	CH ₃	6.90	6.92
49	NH ₂	H	H	3-OH-phenyl	H	CH ₃	7.42	6.93
50	NH ₂	H	Me	phenyl	H	CH ₃	6.82	6.81
51	NH ₂	H	Propargyl	<i>n</i> -Bu	H	CH ₃	6.15	6.65
52	NH ₂	Cl	H	phenyl	H	CH ₃	6.73	6.61
53	NH ₂	F	H	Me	H	CH ₃	7.42	6.71
54	NH ₂	F	H	Et	H	CH ₃	7.51	7.11
55	NH ₂	F	H	<i>n</i> -Bu	H	CH ₃	7.43	7.07
56	NEt ₂	F	H	Et	H	CH ₃	5.78	6.94
57		F	H	Et	H	CH ₃	7.35	7.66
58		F	H	Et	H	CH ₃	7.66	7.58
59		F	H	Et	H	CH ₃	7.62	7.60
60		F	H	Et	H	CH ₃	7.44	7.66
61		F	H	Et	H	CH ₃	7.40	7.52
62		F	H	Et	H	CH ₃	7.10	7.40
63	NH- <i>n</i> -Bu	F	H	Et	H	CH ₃	6.30	6.72

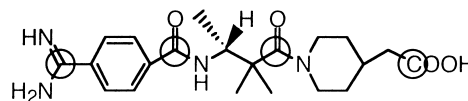
**Figure 1.** Key atoms for alignment. Circled atoms of compound **36** were superposed on the corresponding atoms of all other compounds with optimized conformations.

Table 4. 3D-QSAR equations for inhibitor activity $pIC_{50} = a + [\text{CoMFA}/\text{HINT}/\text{CoMSIA field terms}]$

Methods	<i>a</i>	CN ^a	<i>n</i>	Conventional		Cross-validated ^b		RC ^c			Eq no.
				<i>s</i>	<i>r</i> ²	<i>s</i> _{press}	<i>q</i> ²	St	El	Hp	
CoMFA	3.085	3	63	0.485	0.888	0.774	0.714	80.2	19.8	—	(1)
CoMFA + HINT	3.381	3	63	0.479	0.891	0.766	0.720	44.2	10.4	45.3	(2)
CoMSIA(St + El)	2.962	4	63	0.512	0.877	0.849	0.662	34.2	65.8	—	(3)
CoMSIA(St + El + Hp)	3.437	8	63	0.166	0.988	0.836	0.695	15.3	30.6	54.1	(4)

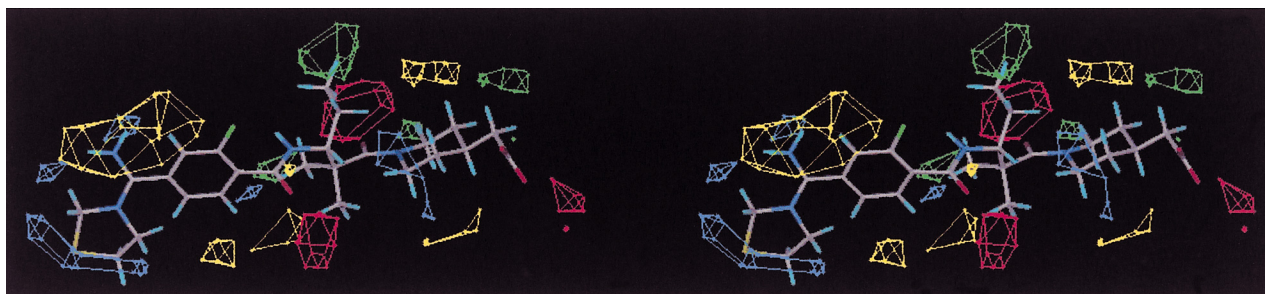
^aNumber of components.^bObtained from the leave-one-out cross-validation.^cRelative contribution (%) of St: steric, El: electrostatic, Hp: hydrophobic effects.

the standard error of estimate and r^2 the correlation coefficient. s_{press} and q^2 are the standard error and the correlation coefficient obtained from the leave-one-out cross-validation, respectively. The quality of the CoMFA-based eqs (1) and (2) in Table 4 was better than the CoMSIA eqs (3) and (4) in terms of the q^2 value and the number of components. Comparing the relative contributions of steric and electrostatic parameters of eq (1) by CoMFA and eq (3) by CoMSIA, steric factors were more important than electrostatic ones in the CoMFA equation while electrostatic interactions were preferred in the CoMSIA equation. Since compounds which are contained in this data set are diverse structurally rather than electrostatically, CoMFA which emphasized steric interactions in this study may provide better results. When HINT was used with CoMFA, the overall statistics of eq (2) were slightly better than those obtained from CoMFA alone (eq (1)). However, the hydrophobic regions, which were drawn according to eqn (2) failed to satisfactorily explain the variations in inhibitory activity. In a previous CoMFA paper about insecticides, we reported that fractions of the hydrophobic term were included within steric and electrostatic field descriptor terms.¹⁴ It is also likely that the hydrophobic field effect is correlated partially with the steric and electrostatic contributions in CoMFA. The pIC_{50} values calculated by eq (1), which was chosen as the best equation, are listed in Tables 1–3.

Figure 2 shows an overlay of the structure of compound **58**, which is the most potent in this study, with the major electrostatic and steric potential contour maps drawn according to eq (1). The red areas in Figure 2 indicate regions where negative electrostatic interactions with the receptor binding site increase the activity,

whereas the blue areas show the reverse case. The green areas in Figure 2 indicate regions where submolecular bulk is well accommodated with an increase in inhibitory activity on fibrinogen binding, whereas the yellow areas indicate regions where submolecular bulk is unfavorable for activity. In the CoMFA field map with compound **58** (Fig. 2), blue positive electrostatic regions on the ligand which are favorable for activity surround the amidino group of compound **58** and red negative electrostatic regions appear near the carboxylate group. These electrostatic fields indicate the importance of cationic and anionic functional groups in the RGD mimetics being favorably located so as to ensure optimal interaction with receptor counterparts. The distance between the center carbon atoms of each amidino and carboxylate group of compound **58**, which is 15.3 Å, appears to be close to the optimum. Negative electrostatic regions above the carbonyl groups adjacent to both the benzene and piperidine rings in compound **58** suggest that electrostatic interactions or hydrogen bonds between these oxygen atoms and the receptor contributes to an increase in activity.

A large sterically forbidden region at the side of one amidino-NH group indicates that the relatively bulky structure at one side is unfavorable for activity, but that the other side is not restricted as is the case for compound **58**. A sterically permissible region around one of the two α -methyl groups of the β -amino acid residue in compound **58** suggests that this methyl group is favorable for a van der Waals interaction with the receptor binding site. A sterically favorable region also locates at the head of the β -ethyl group of the β -amino acid in compound **58**. We previously measured the inhibitory

**Figure 2.** Stereoview of contour diagrams of electrostatic and steric field with compound **58** according to eq (1). See text for an explanation of the colours.

activity for platelet aggregation of RGD X peptides (X = amino acids) and analyzed quantitatively the relationship between the activity and hydrophobicity of the X side chain using our index of the amino acids.¹⁵ The side chain of Trp was the most hydrophobic of natural amino acids and RGDW had the highest activity of the peptides tested. Based on the superposition of compound **58** to RGDW, it appeared that this β -alkyl group corresponded to the Trp side chain of RGDW (figure not shown). Although hydrophobic fields are not involved in CoMFA, a sterically favorable region at the β -ethyl group may be hydrophobic rather than steric. The information obtained in this study should be useful for the design of potent therapeutic drugs for the treatment of thromboses.

References and Notes

1. Marguerie, G. A.; Thomas-Maison, N.; Ginsbarg, M. H.; Plow, E. F. *Eur. J. Biochem.* **1984**, *139*, 5.
2. Ruoslahti, E.; Peirschbacher, M. D. *Science* **1987**, *283*, 491.
3. Miyashita, M.; Akamatsu, M.; Ueno, H.; Nakagawa, Y.; Nishimura, K.; Hayashi, Y.; Sato, Y.; Ueno, T. *Biosci. Biotechnol. Biochem.* **1999**, *63*, 1684.
4. Harada, T.; Katada, J.; Tachiki, A.; Asari, T.; Iijima, K.; Uno, I.; Ojima, I.; Hayashi, Y. *Bioorg. Med. Chem. Lett.* **1997**, *7*, 209.
5. Asari, T.; Ishikawa, S.; Sasaki, T.; Katada, J.; Hayashi, Y.; Harada, T.; Yano, M.; Yasuda, E.; Uno, I.; Ojima, I. *Bioorg. Med. Chem. Lett.* **1997**, *7*, 2099.
6. Hayashi, Y.; Katada, J.; Harada, T.; Tachiki, A.; Iijima, K.; Takiguchi, Y.; Muramatsu, M.; Miyazaki, H.; Asari, T.; Okazaki, T.; Sato, Y.; Yasuda, E.; Yano, M.; Uno, I.; Ojima, I. *J. Med. Chem.* **1998**, *41*, 2345.
7. Cramer, R. D. III.; Patterson, D. E.; Bunce, J. D. *J. Am. Chem. Soc.* **1988**, *110*, 5959.
8. Kellogg, G. E.; Semus, S. F.; Abraham, D. J. *J. Comput.-Aided Mol. Design* **1991**, *5*, 545.
9. Klebe, G.; Abraham, U.; Mietzner, T. *J. Med. Chem.* **1994**, *37*, 4130.
10. SYBYL Molecular Modeling Software, Tripos Associates, Inc., St Louis, MO, USA.
11. Fisher, M. J.; Gunn, B.; Harms, C. S.; Kline, A. D.; Mullaney, J. T.; Nunes, A.; Scarborough, R. M.; Arfsten, A. E.; Skelton, M. A.; Um, S. L.; Utterback, B. G.; Jakubowski, J. A. *J. Med. Chem.* **1997**, *40*, 2085.
12. Stewart, J. J. P. *J. Comput. Chem.* **1989**, *10*, 209, 221.
13. Dewar, M. J. S.; Thiel, W. *J. Am. Chem. Soc.* **1977**, *99*, 4899, 4907.
14. Akamatsu, M.; Nishimura, K.; Osabe, H.; Ueno, T.; Fujita, T. *Pestic. Biochem. Physiol.* **1994**, *48*, 15.
15. Akamatsu, M.; Ueno, T.; Fujita, T. In *Classical and Three-Dimensional QSAR in Agrochemistry*; Hansch, C.; Fujita, T., Eds.; American Chemical Society: Washington, DC, 1995; pp 229–239.